

## Photovoltaic Performance of Naphthol Blue Black Complexes and their Band Gap Energy

Harsasi Setyawati <sup>1\*</sup>, Irminda Kris Murwani <sup>2</sup>, Handoko Darmokoesoemo <sup>1</sup>, Ahmadi Jaya Permana <sup>1</sup>

<sup>1</sup>Department of Chemistry, Faculty of Science and Technology, Airlangga University, Indonesia

<sup>2</sup>Department of Chemistry, Institut Teknologi Sepuluh Nopember, Indonesia

Received 21 April 2022, Revised 7 September 2022, Accepted 26 September 2022

### ABSTRACT

*Along with the depletion of petroleum-based fuels, the development of renewable energy resources is a must. One of them is through DSSC (Dye Sensitized Solar Cells) technology, which has a dye sensitizer and semiconductor as the main components. The aim of this research is to investigate the photovoltaic performance of complexes series from metals (Mn(II); Fe(II); Co(II) and Ni(II)) and naphthol blue-black (NB) as a ligand. This investigation also successfully revealed factors that are highly influencing photovoltaic efficiency, namely the band-gap energy and the conductance of metal-NB complexes. The Fe(II)-NB complex has performed the highest photovoltaic activity as a result of the d-d electron transition and MLCT (Metal to Ligand Charge Transfer) character which are covered by vivid color from the ligand. The bonding between metal and ligand was shown at a wavenumber of 316.33 cm<sup>-1</sup> for M-N bonding and 486.06 cm<sup>-1</sup> for M-O bonding. Fe(II)-NB complex had the narrowest band gap energy which is 5.86 eV and had the highest value of conductance and the highest efficiency, namely 0.0925%. This experiment successfully demonstrates that the narrower the energy gap of a molecule, the ability to transfer electrons is faster. Thus, the efficiency of the solar cell becomes higher. This investigation has proven that the narrow band gap makes the electron transfer becomes easier.*

**Keywords:** band-gap, metal, naphthol-blue-black, photovoltaic, renewable-energy

### 1. INTRODUCTION

The world is currently dealing with the effects of climate change, such as rising global temperatures due to the greenhouse effect, longer and more severe droughts, more extreme tropical storms, and an increase in the frequency of extreme weather events [1-3]. This condition endangers the existence of all living things on Earth. The best way to address this issue is to reduce the primary causes of climate change, namely the use of fossil fuels, and to seek out renewable energy resources. The negative impact of climate change can be mitigated by reducing the use of fossil fuels in all aspects of life. Traditional hydrocarbon fuels could be replaced with an environmentally friendly renewable energy source [4].

On the other hand, the increasing of human population also brings new issues such as, providing energy for their life. The world energy demand is predicted to reach nearly 45 trillion kilo watt hours (kWh) by 2050 [5, 6]. Therefore, the provision of a renewable energy source becomes significant to be done immediately.

Because sunlight is more environmentally friendly than fossil fuels, it has become increasingly important in the production of green energy. The Dye-Sensitized Solar Cell (DSSC) is an outstanding solar cell technology with numerous advantages. DSSC proposes a low fabrication

---

\*Corresponding author: harsasi-s@fst.unair.ac.id

budget, is easily modified, eco-friendly, and highly efficient [7]. DSSC cells are made up of semiconductors, dye sensitizers, conductive glass for the cell body, and electrolyte solution [8-10]. Because of the importance of semiconductor and dye sensitizers in DSSC performance, many researchers are focusing on their development.

This study concentrated on improving dye sensitizer performance because it is an important photon harvester of sunlight [9, 11]. Metal complexes were developed as dye sensitizers on DSSC in this project because the dye sensitizer material from metal complexes is easy to modify the band gap [12]. The metal complexes were synthesized from the metal centers of Mn(II), Fe(II), Co(II), Ni(II), and the ligand naphthol blue-black (NB), wherein the metal complexes will be written as Mn-NB, Fe-NB, Co-NB, and Ni-NB in the rest of the article. Ligand NB was chosen because it contains a chromophore group, allowing the NB to harvest photons from sunlight [9]. On the other hand, the metal center with the lowest oxidation number was chosen so that the resulting metal complexes have a significant character for the electron transfer process known as Metal Ligand Charge Transfer (MLCT). Because of its good ability to harvest energy from sunlight, a metal complex with MLCT character is preferable and usable as a dye sensitizer on DSSC [13-15].

This experiment finally synthesized and characterized a series of metal-NB complexes, investigated their photovoltaic performance, and determined their band gap energy to analyze factors that determine that metal complex's photovoltaic trait. The wavelength and band gap of metal complexes were investigated, as well as their wavenumber and functional group and conductance value. Fluorine thin oxide (FTO) was used as a conductive glass, titanium dioxide (TiO<sub>2</sub>) as a semiconductor, and potassium iodide (KI<sub>3</sub>) as an electrolyte solution in this study.

## 2. MATERIAL AND METHODS

### 2.1 Materials

Materials which were used in this probe were provided by Sigma Aldrich. There are naphthol blue black (C<sub>22</sub>H<sub>14</sub>N<sub>6</sub>Na<sub>2</sub>O<sub>9</sub>S<sub>2</sub>; 80%), manganese sulfate salt (MnSO<sub>4</sub>), Mohr salt [(NH<sub>4</sub>)<sub>2</sub>Fe(SO<sub>4</sub>)<sub>2</sub>·6H<sub>2</sub>O], cobalt(II)chloride dihydrate (CoCl<sub>2</sub>·2H<sub>2</sub>O), nickel sulfate hydrate (NiSO<sub>4</sub>·7H<sub>2</sub>O), ethanol (C<sub>2</sub>H<sub>5</sub>OH; Merck, 99%), I<sub>2</sub> solution in potassium iodide (KI), titanium tetraisopropoxide (TTIP; 97%), Triton X-100 (C<sub>14</sub>H<sub>22</sub>O(C<sub>2</sub>H<sub>4</sub>O)<sub>4</sub>); Merck, 98%), hydrochloric acid (HCl), acetic acid (CH<sub>3</sub>COOH), ethanol (C<sub>2</sub>H<sub>5</sub>OH), and aquabides.

### 2.2 Synthesis of Metal-NB Complexes

All metal-NB complexes were synthesized based on the mole ratio of metal: naphthol blue-black (ligand) which was 1:3. To begin with, one mole metal and three mole naphthol blue-black powder were weighed. After that, ethanol was used to dissolve metals and naphthol blue-black. The metal solutions were then combined with naphthol blue black solution, agitated for a quarter hour, and then refluxed for 90 minutes at temperature of 78 °C. In the next step, each metal-NB complex solution was heated until the solution was reduced to one third. After a solid of metal complex was obtained, the precipitate was separated from the solution by filtering via a Buchner funnel, purified by using hot ethanol, and the last step was to let the sample dry [9].

### 2.3 Characterization of Metal-NB Complexes

In this project, UV-VIS spectrophotometer was used to analyze the absorption band characteristics and to determine the band gap energy of metal-NB complexes. A Fourier Transform Infra-Red (FTIR) spectrophotometer was utilized to investigate bonding between

metal and ligand NB structure. A conductometer was operated to determine the ability of metal-NB complexes in conducting ion or electrons (the electrical conductivity).

## 2.4 Determination Band Gap Energy of Metal-NB Complexes

The metal-NB complexes were weighed 0.001 gram, dissolved in distilled water, and diluted with ethanol to the mark in a 10 ml volumetric flask. Band gap energy is determined by calculating the absorbance of complex compounds at a wavelength of 200-800 nm with a range of 1 nm using a UV-Vis spectrophotometer first. After that, the Tauc graph plot method is applied by drawing a linear line to intersect the X axis on the graph of the relationship between  $h\nu$  and  $(\alpha h\nu)^2$  [16]. Where  $h$  is Planck constant ( $6,626 \times 10^{-34}$  Js =  $4,136 \times 10^{-34}$  eV);  $\nu$  = beam frequency (Hz);  $\alpha$  = absorption coefficient).

## 2.5 Determination Photovoltaic Performance of Metal-NB Complexes

### 2.5.1 Semiconductor preparation on DSSC from titanium dioxide

Titanium dioxide was prepared by the sol gel method. Firstly, 5 ml of Triton X-100 was added to 12 ml of acetic acid. Then, the solution was added by 225 ml of ethanol while being stirred for five minutes. In another glass beaker, 15 ml solution of  $\text{TiO}_2$  precursor namely Titanium isopropoxide (TTIP) was solvated by 1 ml of hydrochloric acid. After that, the Triton X-100 and TTIP solution were blended and stirred for a two hours until the formation of sol. The sol could then be layered on the conductive glass [9].

### 2.5.2 Preparation of a working electrode and a counter electrode on DSSC

For a working electrode, a  $10^{-2}$  M solution of the metal-NB complexes was used to submerge the  $\text{TiO}_2$ -coated glass plate for 24 hours. This must be done so that the metal-NB complex is immersed homogeneously on a glass plate. Firstly, the glass plate was placed in a dark, tightly covered container to prevent scratches from damaging the  $\text{TiO}_2$  coating. Secondly, the glass plate's surface was covered with carbon allotropy (graphite) that produced by a graphite pencil for a counter electrode. Lastly, a counter electrode re-covered with carbon from wax smoke uniformly [9].

### 2.5.3 Fabricating process of DSSC cells

First of all, the previously made working electrode was placed on a table in a position where the naphthol blue black complex compound was placed on top. Next, the counter electrode was placed in front of the working electrode. Note that there should be no air bubbles in the  $\text{I}_2$  in KI solution in the electrode. The clamping clips were properly arranged to maintain the composition of the glass plate together. Then the DSSC series were connected to a multimeter, with the positive (+) pole connected to the counter electrode and the negative (-) pole connected to the DSSC work electrode. Finally, the maximum voltage and current were determined. The measurement was taken place when the sun is present. The intensity of the sun's radiation was then measured with a luxmeter [7].

## 3. RESULTS AND DISCUSSION

Metal-NB complex compounds were created by reacting metals in a 1:3 mole ratio with naphthol blue-black (as a ligand). Following that, all obtained solids were characterized using a UV-VIS

spectrophotometer, FTIR, and conductometer. Finally, all metal complexes were used as dye sensitizer materials on DSSC cells. The photovoltaic performances of metal-NB complexes were determined and compared. The factors that influenced the most the photovoltaic characteristics were investigated

### 3.1 The Result of Metal-NB Complexes Characterization

The first characterization was using UV-VIS spectrophotometer to determine the characteristic of absorption band and band gap of the metal-NB complex. The result has been tabled in Table 1. The appearance band in the UV region (under 400 nm) on metal-NB complex represents the Metal to Ligand Charge Transfer (MLCT) phenomenon. MLCT is the process of electron transfer from metal (M) to a ligand (L) and only occurs in the metal complex. The MLCT transition weakens the binding of the ligand and strengthens the metallic bond with the ligand [17, 18]. Complex compounds that experience the MLCT phenomenon are promising to be applied as dye sensitizers in the solar cells because they have a "light-harvesting" characteristic which can absorb more sunlight to be converted into electrical energy [13, 15, 19]. From Table 1, we can also conclude that the d-d transition band of all complexes is obscured by the maximum wavelength of naphthol blue-black and occurs at 616-619 nm.

**Table 1** Characteristics band of naphthol blue black (NB) and the metal-NB complexes

Compound	Wavelength (nm)		
<b>NB</b>	228	-	619
<b>Mn-NB</b>	231	272.5 **	617*
<b>Fe- NB</b>	233	273.5**	618*
<b>Co-NB</b>	224	272**	616*
<b>Ni-NB</b>	227	266, 272**	616*
<b>*d-d transition</b>	<b>**MLCT band</b>		

The second characterization was using FTIR to determine the functional group and the metal-ligand bond on the metal-NB complexes. The spectra and the detail of the wavenumber are shown in Figure 1 and Table 2. According to Figure 1, we can see that the spectra of the metal complexes are not significantly different from those of the NB ligand. This indicates that naphthol blue black as a ligand remains intact and undamaged during the complexation process. This condition is very beneficial because the structure of the ligand significantly contributes to the photon capture capability of the material dye sensitizer. The binding of metal to ligand in complex compounds can be determined by comparing the FTIR spectrum of naphthol blue black with the synthesized complex compound. Table 2 shows that all metal-ligand bonding occurred through M-N and M-O bonding and appear at wavenumbers below 600  $\text{cm}^{-1}$ . Bonding between M-N for Mn-NB is shown at 308.61  $\text{cm}^{-1}$ ; 316.33  $\text{cm}^{-1}$  for Fe-NB; 324.40  $\text{cm}^{-1}$  for Co(II)-NB and 354.90  $\text{cm}^{-1}$  for Ni-NB. On the other hand, M-O bonding for Mn-NB is shown at 540.07  $\text{cm}^{-1}$ ; 486.06  $\text{cm}^{-1}$  for Fe-NB; 354.90  $\text{cm}^{-1}$  for Co-NB and 486.06  $\text{cm}^{-1}$  for Ni-NB. The appearance of the metal-ligand bonds across the M-N and M-O bonds indicates that the metals and ligand in the metal-NB complex are chemically bound. It is beneficial in facilitating electron flow in DSSC cell performance [20].

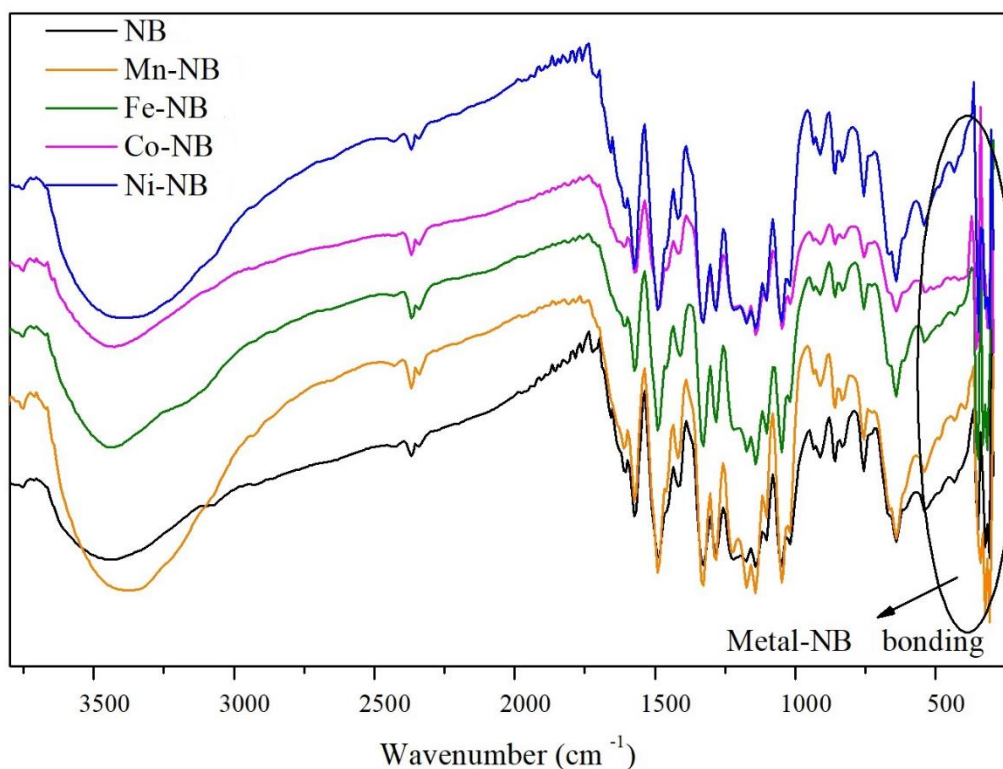


**Figure 1.** FTIR spectra of ligand NB and metal-NB complexes

**Table 2** Table of functional group from ligand NB and the metal-NB complexes

Functional Groups	Wavenumber (cm <sup>-1</sup> )					Theoretical and reference
	NB	Mn-NB	Fe-NB	Co-NB	Ni-NB	
M-N	-	308.61	316.33	324.40	354.90	400 - 300 [21]
M-O	-	540.07	486.06	354.90	486.06	600 - 400 [21]
SO <sub>3</sub> Na	1141.86	1103.28	1141.86	1172.72	1141.86	1235 - 1070 [22]
N=N	1419.61	1419.61	1411.89	1419.61	1419.61	1500 -1400 [23]
NO <sub>2</sub>	1489.05	1489.05	1489.05	1489.05	1489.05	1550 -1300 [23]
C=C aromatic	1573.91	1573.91	1573.91	1573.91	1573.91	1607- 1510 [23]
OH	3441.01	3371.57	3425.58	3425.58	3425.58	3639 - 3029 [22]
NH from primer amine	3749.62	3749.62	3749.62	3749.62	3749.62	3800 - 3300 [24]

### 3.2 The Result of Band Gap Energy of Metal-NB Complexes Determination

The bandgap energy of metal-NB complexes is then determined by measuring the absorbance of each complex compound solution. The results of absorbance, absorption coefficient  $\alpha$ , and energy  $h\nu$  of the metal-NB complex were used to calculate the energy  $h\nu$  and  $(\alpha h\nu)^2$  in order to determine the bandgap energy of each complex. Figure 2 depicts the bandgap curves of each complex compound. Complex Mn-NB has a bandgap energy of 5.87 eV, complex Fe-NB has a bandgap energy of 5.86 eV, complex Co-NB has a bandgap energy of 5.93 eV, and complex Ni-NB has a bandgap energy of 5.87 eV, according to Figure 2. Because the electron will excite more easily due to the closer distance between Highest Occupied Molecular Orbital (HOMO) and Lowest Unoccupied Molecular Orbital (LUMO), the complex's conductivity value will increase. [25-29]. The results of the conductivity determination described in Table 3 support this assertion. The Fe-

NB complex has the highest conductance,  $59.6 \text{ ohm}^{-1}$ , as shown in Table 3. The smaller the bandgap energy, the closer the HOMO-LUMO bands are to one another, and thus the higher the conductance value. This makes the electron injection process easier, resulting in faster electron flow and higher electric current generation. [30, 31].

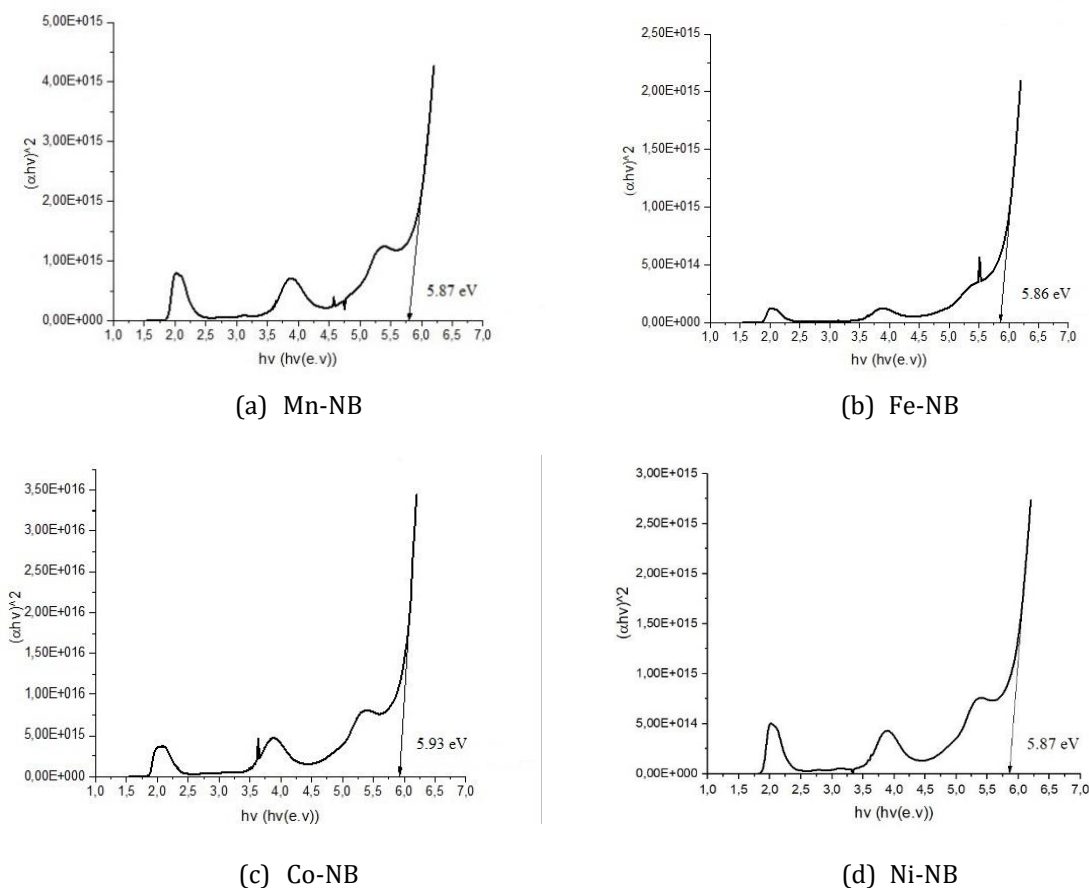


**Figure 2.** Bandgap energy of metal-NB complexes

**Table 3** Conductance value of metal-NB complexes

Compound	Water	Mn-NB	Fe-NB	Co-NB	Ni-NB
Conductance ( $\text{ohm}^{-1}$ )	1.98	18.27	59.6	24.10	21.70

### 3.3 The Result of Determination Photovoltaic Performance of Metal-NB Complexes

In this study, the photovoltaic performance of metal-NB complexes as dye sensitizers was compared to the NB itself as a ligand. In Table 4, it can be compared that the Fe-NB complex produces the highest efficiency than the other complex, namely 0.0925 %. The greater efficiency value indicates that the compound has a better ability in converting solar energy into electrical energy [32]. Fe-NB complex shows higher photovoltaic performance because the electron regeneration process occurs easily due to having the narrowest band gap energy and the highest conductance value. The narrowest band gap energy of the metal-complex represents that the distance of the HOMO-LUMO band is very close or small [33]. This condition is preferable because

it can make electrons easier to transport when the DSSC cell is working. This explanation is strengthened by the conductance value in Table 3. The distance between of the HOMO-LUMO band of complex Fe-NB is the narrowest. It makes the electron moves smoothly so that the conductance value becomes high. Besides, the MLCT characteristic that possessed by Fe-NB also contributes in supporting its photovoltaic performance. The presence of the MLCT phenomenon on the metal-NB complex will strengthen the bonding between metal and ligand, so the metal complex will have a good ability in capturing the energy photons from sunlight [13, 18]. The more photons from sunlight are being captured, the higher efficiency of the solar cell will be obtained.

Finally, the findings of this study demonstrate that a molecule's band gap distance has a significant impact on the electron transfer process in a solar cell system. The higher the photovoltaic efficiency produced by solar cells, the easier or simpler the electron transfer process in solar cell devices is.

Table 4 Photovoltaic performance variable of NB and metal-NB complexes

Compound	V <sub>oc</sub> (V)	J <sub>sc</sub> (mA/cm <sup>2</sup> )	FF	η (%)
NB	0.2180	0.0240	0.7844	0.0083
Mn-NB	0.0380	0.1843	0.8930	0.0126
Fe-NB	0.3630	0.1418	0.8887	0.0925
Co-NB	0.0356	0.1643	0.9087	0.0107
Ni-NB	0.0445	0.2508	0.6865	0.0155
Sunlight = 49.44 (watt/cm <sup>2</sup> )				

#### 4. CONCLUSION

The photovoltaic performance of series metal-NB complexes has been successfully demonstrated. The MLCT phenomenon, band gap energy, and complex conductance value were the main factors that affected the photovoltaic performance of metal-NB complexes. Complex Iron-NB demonstrated the best photovoltaic performance, as evidenced by the highest efficiency value of 0.0925 %. In a short circuit, Fe-NB produces a current of 0.567 mA/cm<sup>2</sup> and the maximum voltage of 0.363 V.

#### ACKNOWLEDGEMENTS

This research has been supported by the Ministry of Research, Technology and Higher Education (RISTEKDIKTI) Indonesia through the Grant "Penelitian Dasar" also Faculty of Science and Technology, Airlangga University, Surabaya, Indonesia through the Grant "Penelitian Unggulan Fakultas" and Chemistry Department, Faculty of Science and Technology, Airlangga University Surabaya, Indonesia for all support.

#### REFERENCES

- [1] D. Osberghaus, C.J.G.E.C. Fugger, Natural disasters and climate change beliefs: The role of distance and prior beliefs, 74 (2022) 102515.
- [2] J. Pearce-Higgins, L. Antão, R. Bates, K. Bowgen, C.D. Bradshaw, S. Duffield, C. Ffoulkes, A. Franco, J. Geschke, R.J.E.i. Gregory, A framework for climate change adaptation indicators for the natural environment, 136 (2022) 108690.

- [3] D. Scavia, J.C. Field, D.F. Boesch, R.W. Buddemeier, V. Burkett, D.R. Cayan, M. Fogarty, M.A. Harwell, R.W. Howarth, C.J.E. Mason, Climate change impacts on US coastal and marine ecosystems, 25 (2002) 149-164.
- [4] A. Olabi, M.A.J.R. Abdelkareem, S.E. Reviews, Renewable energy and climate change, 158 (2022) 112111.
- [5] D.L. Greene, J.L. Hopson, J.J.E.P. Li, Have we run out of oil yet? Oil peaking analysis from an optimist's perspective, 34 (2006) 515-531.
- [6] R. Newell, D. Raimi, G.J.R.f.t.F. Aldana, Global energy outlook 2019: the next generation of energy, 1 (2019) 8-19.
- [7] H. Setyawati, H. Darmokoesoemo, A.T.A. Ningtyas, Y. Kadmi, H. Elmsellem, H.S.J.R.i.p. Kusuma, Effect of metal ion Fe (III) on the performance of chlorophyll as photosensitizers on dye sensitized solar cell, 7 (2017) 2907-2918.
- [8] M.B. Qadir, K.C. Sun, I.A. Sahito, A.A. Arbab, B.J. Choi, S.C. Yi, S.H.J.S.E.M. Jeong, S. Cells, Composite multi-functional over layer: A novel design to improve the photovoltaic performance of DSSC, 140 (2015) 141-149.
- [9] H. Setyawati, H. Darmokoesoemo, I. Murwani, Dye-sensitized solar cells with naphthol blue black as dye sensitizer, Journal of Physics: Conference Series, IOP Publishing, 2021, pp. 032016.
- [10] H. Setyawati, H. Darmokoesoemo, F. Rochman, A.J.J.M.f.R. Permana, S. Energy, Affordable dye sensitizer by waste, 6 (2017) 1-6.
- [11] H. Setyawati, M. Hadi, H. Darmokoesoemo, I. Murwani, A. Permana, F. Rochman, Modification of Methyl Orange dye as a light harvester on solar cell, IOP Conference Series: Earth and Environmental Science, IOP Publishing, 2020, pp. 012010.
- [12] T. Jiang, G. Zhang, R. Xia, J. Huang, X. Li, M. Wang, H.-L. Yip, Y.J.M.T.E. Cao, Semitransparent organic solar cells based on all-low-bandgap donor and acceptor materials and their performance potential, 21 (2021) 100807.
- [13] A.B. Athanas, S.J.A.E. Kalaiyar, S. Research, Quinoline-Coupled Coumarin-Based Ruthenium (II) Dye Sensitizer for Photoelectrochemical Cells and Solar Cells: A Mimic for an Artificial-Light-Harvesting System, 2 (2021) 2100094.
- [14] H. Darmokoesoemo, A.R. Fidyayanti, H. Setyawati, H.S.J.K.C.E.R. Kusuma, Synthesis of complex compounds Ni (II)-chlorophyll as dye sensitizer in dye sensitizer solar cell (DSSC), 55 (2017) 19-26.
- [15] B.S. Shivaji, T. Swetha, T. Gayathri, S.P.J.S.A.P.A.M. Singh, B. Spectroscopy, Aza-dipyrinato Ruthenium Sensitizers for Enhancement of Light-Harvesting Ability of Dye-Sensitized Solar Cells, (2022) 121131.
- [16] M.K. Hossain, A. Mortuza, S. Sen, M. Basher, M. Ashraf, S. Tayyaba, M. Mia, M.J.J.O. Uddin, A comparative study on the influence of pure anatase and Degussa-P25 TiO<sub>2</sub> nanomaterials on the structural and optical properties of dye sensitized solar cell (DSSC) photoanode, 171 (2018) 507-516.
- [17] P.C. Servaas, D.J. Stufkens, A.J.I.C. Oskam, Spectroscopy and photochemistry of nickel (0)-alpha-diimine complexes. 1. Structural differences among NiL<sub>2</sub> and Ni (CO) 2L (L= alpha-diimine) complexes: molecular orbital calculations and an electronic absorption and resonance Raman study, 28 (1989) 1774-1780.
- [18] X. Zhang, S.E. Canton, G. Smolentsev, C.-J. Wallentin, Y. Liu, Q. Kong, K. Attenkofer, A.B. Stickrath, M.W. Mara, L.X.J.J.o.t.A.C.S. Chen, Highly accurate excited-state structure of [Os (bpy) 2dcbpy] 2+ determined by X-ray transient absorption spectroscopy, 136 (2014) 8804-8809.
- [19] G. Miessler, P. Fischer, D. Tarr, Inorganic chemistry fifth edition, New York: Pearson Education, Inc, 2014.
- [20] J. Wang, Z. Cai, D. Lin, K. Chen, L. Zhao, F. Xie, R. Su, W. Xie, P. Liu, R.J.A.A.M. Zhu, Interfaces, Plasma Oxidized Ti<sub>3</sub>C<sub>2</sub>T<sub>x</sub> MXene as Electron Transport Layer for Efficient Perovskite Solar Cells, 13 (2021) 32495-32502.



- [21] K. Nakamoto, Infrared and Raman spectra of inorganic and coordination compounds, part B: applications in coordination, organometallic, and bioinorganic chemistry, John Wiley & Sons 2009.
- [22] J.C. Greever, Organic Chemistry, (Fessenden, Ralph J.; Fessenden, Joan S.), ACS Publications, 1995.
- [23] J. Workman Jr, The handbook of organic compounds, three-volume set: Infrared, ultraviolet, and visible spectra featuring polymers and surfactants, Elsevier 2000.
- [24] A.D. Khalaji, S. Mehrani, V. Eigner, M.J.J.o.M.S. Dusek, Synthesis, experimental and theoretical studies on its crystal structure and FT-IR spectrum of new thiosemicarbazone compound E-2-(4-isopropylbenzylidene) thiosemicarbazone, 1047 (2013) 87-94.
- [25] A.H. Ahmed, A. Hassan, H.A. Gumaa, B.H. Mohamed, A.M. Eraky, A.A.J.A.J.o.C. Omran, Copper (II)-oxaloyldihydrazone complexes: Physico-chemical studies: Energy band gap and inhibition evaluation of free oxaloyldihydrazone toward the corrosion of copper metal in acidic medium, 12 (2019) 4287-4302.
- [26] M.-L. Fu, G.-C. Guo, X. Liu, B. Liu, L.-Z. Cai, J.-S.J.I.C.C. Huang, Syntheses, structures and properties of three selenoarsenates templated by transition metal complexes, 8 (2005) 18-21.
- [27] M.K. Ghosh, S. Pathak, T.K.J.A.o. Ghorai, Synthesis of two mononuclear schiff base metal (M= Fe, Cu) complexes: MOF structure, dye degradation, H<sub>2</sub>O<sub>2</sub> sensing, and DNA binding property, 4 (2019) 16068-16079.
- [28] S.K. Sengupta, O.P. Pandey, B.K. Srivastava, V.K.J.T.m.c. Sharma, Synthesis, structural and biochemical aspects of titanocene and zirconocene chelates of acetylferrocenyl thiosemicarbazones, 23 (1998) 349-353.
- [29] N. Turan, B. Gündüz, H. Körkoca, R. Adigüzel, N. Çolak, K.J.J.o.t.M.C.S. Buldurun, Study of structure and spectral characteristics of the Zinc (II) and Copper (II) complexes with 5, 5-Dimethyl-2-(2-(3-nitrophenyl) hydrazono) cyclohexane-1, 3-dione and their effects on optical properties and the developing of the energy band gap and investigation of antibacterial activity, 58 (2014) 65-75.
- [30] R. Katoh, A.J.J.o.P. Furube, P.C.P. Reviews, Electron injection efficiency in dye-sensitized solar cells, 20 (2014) 1-16.
- [31] M.M. Moharam, A.N. El Shazly, K.V. Anand, D.E. Rayan, M.K. Mohammed, M.M. Rashad, A.E.J.T.i.C.C. Shalan, Semiconductors as effective electrodes for dye sensitized solar cell applications, 379 (2021) 1-17.
- [32] R. Tarsang, V. Promarak, T. Sudyoadsuk, S. Namuangruk, S.J.J.o.P. Jungsuttiwong, P.A. Chemistry, Tuning the electron donating ability in the triphenylamine-based D- $\pi$ -A architecture for highly efficient dye-sensitized solar cells, 273 (2014) 8-16.
- [33] B.G. Kim, X. Ma, C. Chen, Y. Ie, E.W. Coir, H. Hashemi, Y. Aso, P.F. Green, J. Kieffer, J.J.A.F.M. Kim, Energy level modulation of HOMO, LUMO, and band-gap in conjugated polymers for organic photovoltaic applications, 23 (2013) 439-445.

